Article ID: 1003－6326(2003)01－0140－05

Microstructure and properties of composite of stainless steel and partially stabilized zirconia①

ZHANG Wen-quan(张文泉)[1, 2], XIE Jian-xin(谢建新)[1], YANG Zhi-guo(杨志国)[1], WANG Cong-zeng(王从曾)[2]

(1. School of Materials Science and Engineering, University of Science and Technology Beijing, Beijing 100083, China;
2. School of Materials Science and Engineering, Beijing Polytechnic University, Beijing 100022, China)

Abstract: To fabricate the metal-ceramics multi-layer hollow functionally gradient materials(FGMs) that might meet the requirement of repeated service and long working time of high temperature burners, such as spacecraft engine, the microstructure and properties of composite of stainless steel and partially stabilized zirconia were investigated. Samples of different proportions of stainless steel to partially yttria-stabilized zirconia were fabricated by powder extrusion and sintering method. Shrinkage, relative density, microstructure, micro-Vickers hardness, compression strength, bending strength, fractography morphology and electrical resistivity of sintered samples with different proportions of stainless steel were measured. The results show that threshold of metallic matrix composite(MMC) is approximately equal to 60% (volume fraction) stainless steel. The samples with 0 to 50% (volume fraction) stainless steel indicate ceramic brittleness and non-cutability, and the samples with 70% to 100% (volume fraction) stainless steel indicate metallic plasticity and cutability.

Key words: functionally gradient materials; high temperature burner; composite; stainless steel; zirconia; threshold

CLC number: TG 142 **Document code:** A

1 INTRODUCTION

Owing to the requirements of repeated service and long working time of high temperature burners, such as spacecraft engine, the material of the burners should have good structure processability, as well as high temperature resistance, thermal shock resistance and thermal fatigue resistance[1, 2]. In this connection, functionally gradient materials (FGMs) were developed widely[1-6]. Having compared with several processing methods, the authors proposed to develop a kind of multi-layer metal-ceramics tube(Fig. 1) to meet such special requirements utilizing the multi-billet extrusion forming and sintering solidification[7, 8]. The extrusion characteristics of mixed powder of stainless steel and partially stabilized zirconia(PSZ) were known in previous works[9-11]. In order to design and fabricate optimum thermal stress relieved multi-layer metal-ceramics tube, the microstructure and properties for sintered rods of different proportions of stainless steel(316L) to partially yttria-stabilized zirconia(3% Y_2O_3(mole fraction)-PSZ) are investigated. Shrinkage, relative density, microstructure, micro-Vickers hardness, compression strength, bending strength, fractography morphology and electrical resistivity of gas-pressure sintered samples with different proportions of stainless steel were measured, and the results are also discussed.

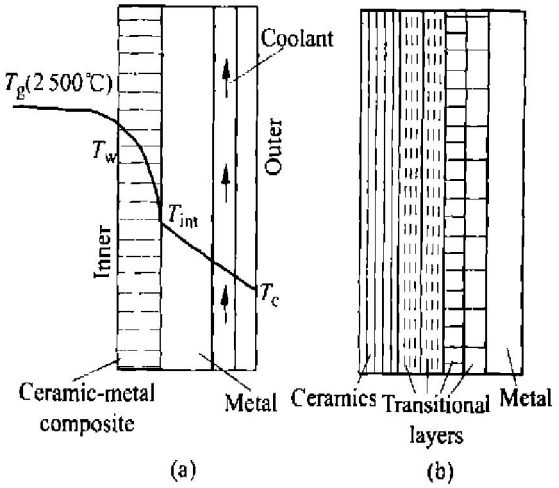

Fig. 1 Material design for high temperature burner
(a) —Wall of burner; (b) —Ceramic-metal composite

2 EXPERIMENTAL

Atomic stainless steel(316L) powder with average

① **Foundation item:** Project(59671025) supported by the National Natural Science Foundation of China; project supported by the State Key Laboratory of Powder Metallurgy of China **Received date:** 2002－01－05; **Accepted date:** 2002－05－08

Correspondence: Prof. Xie Jian-xin, School of Materials Science and Engineering, University of Science and Technology Beijing, Beijing 100083, China; Tel: +86-10-62332254, 62333999; Fax: +86-10-62334311; E-mail: jxxie@mater.ustb.edu.cn

particle diameter 5~ 10 μm, partially stabilized zirconia (PSZ) containing 3% yttria(mole fraction) and with average diameter 0. 45 μm and the binder of 10% slurry (mass fraction) of hydroxy-propyl methyl-cellulose (HPMC) powder and purified water were used in the experiment.

Mixtures of 316L powder and PSZ powder (MoP) containing 0, 10%, 30%, 50%, 60%, 70%, 80%, 90% and 100% (volume fraction) of 316L, respectively, were fabricated. Then, the MoPs were mixed with the binder of 10% HPMC' mass to get plastic mixtures of powder(PMoP). After aging for 24 h under airtight sealing, the nine different PMoPs were extruded into rods of *d* 6. 7 mm or *d* 4. 7 mm, respectively, under constant extrusion speed of 0. 167 mm/s at room temperature by an extruder of diameter of 15 mm.

Water was removed from the as-extruded samples by drying in air for 24 h at room temperature and at 110 ℃ for 1 h in sequence. Then, the binder was removed at 450 ℃ for 4 h for the *d* 6. 7 mm rods and at 400 ℃ for 3 h for the *d* 4. 7 mm rods, followed by the gas-pressure sintering scheme as illustrated in Fig. 2 to get sintered rods.

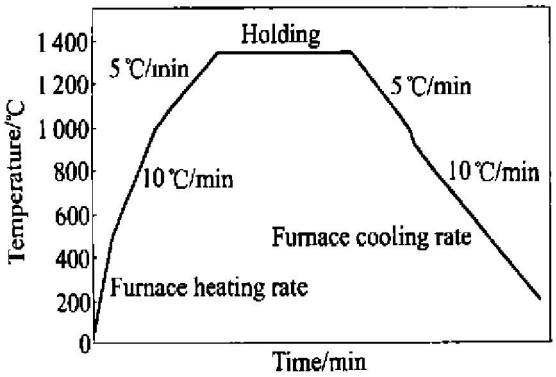

Fig. 2 Scheme of sintering
(Initial vacuum 8 Pa; at 1 350 ℃, holding for 80 min in vacuum, then 70 min in argon gas of 9 MPa)

In order to avoid being molten of 316L in sintering, sintering temperature should be below 1 400 ℃. On the other hand, this sintering temperature below 1 400 ℃ is relatively low for densification of PSZ. Therefore, the gas-pressure sintering technology at 1 350 ℃ was utilized.

Analytical measurements of 1) the linear shrinkage ψ of rod diameter and relative density ρ_r, 2) microstructure by means of optical microscope and SEM microscope, 3) micro-Vickers hardness $HMV_{0.2/15}$ (load: 1. 961 N, holding time: 15 s) of PSZ matrix and 316L particles, and 4) compression strength σ_{bc} (compression platens speed: 0. 016 7 mm/s) were conducted for the *d* 6. 7 mm sintered rods; and three-bending strength σ_{bb} (span: 24 mm, crosshead speed: 6. 67 μm/s), fractography morphology (SEM) and electrical resistivity ρ (utilizing Kelvin bridge) were also conducted for the *d* 4. 7 mm sintered rods.

3 RESULTS AND DISCUSSION

3.1 Variation of shrinkage ψ and relative density ρ_r

The relative density of the as-extruded rods (after drying and debindering) ρ_{r0} varies with increasing 316L proportion in the composite, as shown in Fig. 3, which is caused by the particle size distribution of powder mixture. The difference of relative density of the as-extruded rods ρ_{r0} leads to the reverse variation of the shrinkage ψ of sample diameter with increasing 316L in the composite, as shown in Fig. 3. Both the relative density of the as-extruded rods ρ_{r0} and the sintering shrinkage ψ affect the relative density ρ_r of sintered samples. The variation of the two factors is reverse as the variation of 316L proportion, and the relative density of the as-extruded rods ρ_{r0} is more effective than the shrinkage ψ. Therefore, the variation of ρ_r is relatively similar to that of the relative density ρ_{r0} of the as-extruded rods.

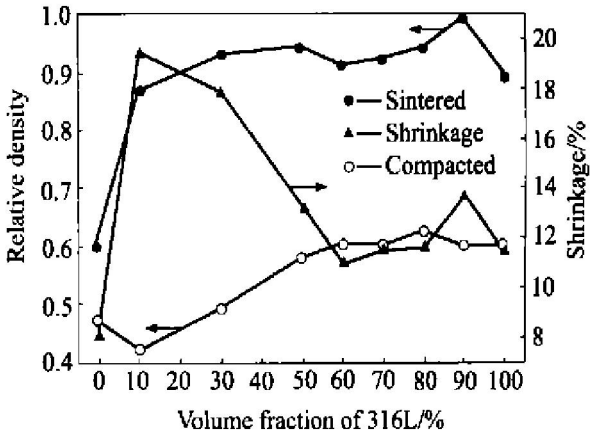

Fig. 3 Variation of shrinkage and relative density with volume fraction of 316L

3.2 Microstructure

The amounts of porosity in the PSZ matrix of the sintered samples of 10%, 30% and 50% 316L are relatively small by contrast to that of the others. In other words, the PSZ matrix of the three kinds of the sintered samples is denser than that of the others. In the samples of 10% and 30% 316L, 316L particles disperse among PSZ matrix. With increasing 316L proportion from 50% (volume fraction), 316L particles get inter-bonding and coalescence and coarsening, and form framework gradually. For example, microstructure of 90% 316L is described as the continuous 316L framework dispersed with not fully dense PSZ inclusions, as shown in Fig. 4(a). In a word, the matrix is the 316L framework in the sintered samples with more than 60% 316L(volume fraction), while the matrix is inter-bonding and coalescence PSZ particles in those

with less than 60% 316L. As a result, the threshold[12, 13] of the metallic matrix composite(MMC) is approximately equal to 60% volume fraction of stainless steel, as shown in Fig. 4(b).

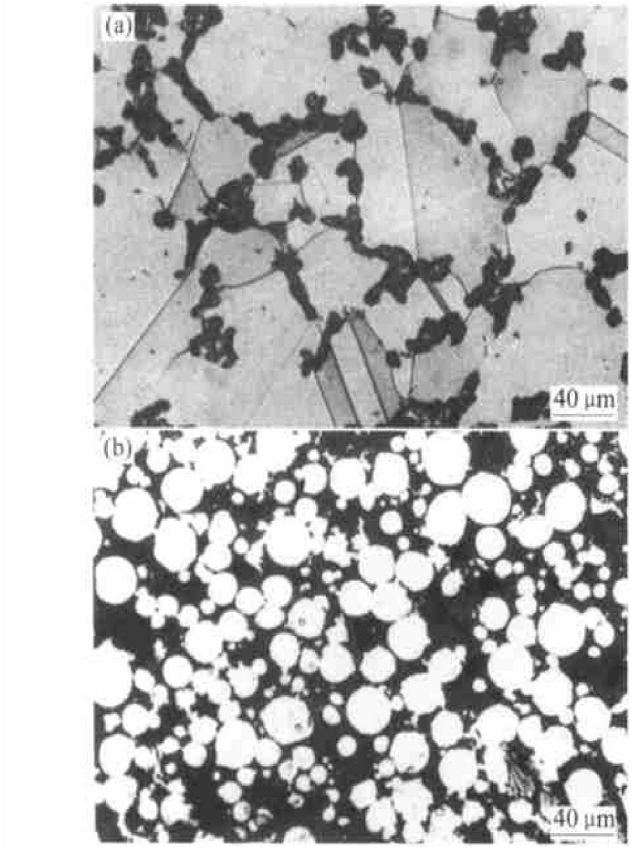

Fig. 4 Optical images of typical composites
(a) —90% volume fraction of 316L(etched)
(b) —60% volume fraction of 316L;

3.3 Mechanical properties and fracture morphology

As illustrated in Fig. 5, the micro-Vickers hardness $HMV_{0.2/15}$(GPa) of the PSZ matrix rises gradually up to 30% 316L(volume fraction), then drops gradually, while $HMV_{0.2/15}$ of 316L particles varies unnoticeably over the whole range of 316L proportion. The variation of $HMV_{0.2/15}$ of PSZ matrix represents that of the densification of the PSZ matrix with the variation of 316L proportion. The tendency is not exactly consistent with that of the relative density, since the relative density is the average of the composites. Sintered samples do not possess cutability until 316L proportion increases to 60%, which is exactly consistent with above microstructure observation.

As shown in Fig. 6, compression strength σ_{bc} rises slightly until 316L proportion increases to 60%, then rises appreciably, which is slightly consistent with the above variation of the relative density. From 0% to 60% 316L, the fracture of the compressive testing is approximately longitudinal along the axis of the cylindrical samples, which indicates typical brittleness. In contrast, the fractures of the samples from 70% to 90% 316L make an approximate angle of 45° with the compressive direction, which indicates typical metallic plasticity. In addition, during compressive testing 100% 316L samples are only upset into discs, and no rupture appears. Since 60% of 316L is approximately equal to the threshold of the metallic matrix composite(MMC), the samples of 60% 316L possess cutability, but still indicate brittleness fracture during the compressive testing. In a word, 60% 316L samples have transitional character between metal and ceramics. This noticeable character, which is consistent with the above microstructure observation, is extremely valuable to further optimum design about composition and structure of multi-layer hollow functionally gradient materials.

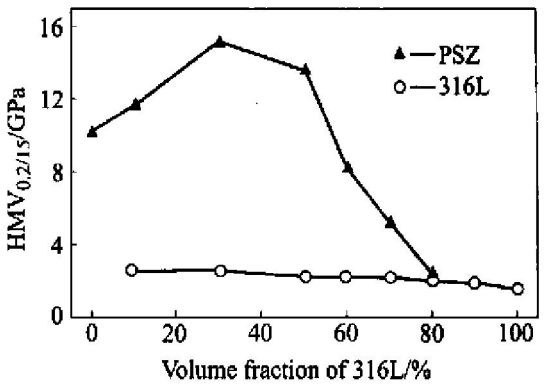

Fig. 5 Relationship between micro-Vickers hardness and volume fraction of 316L

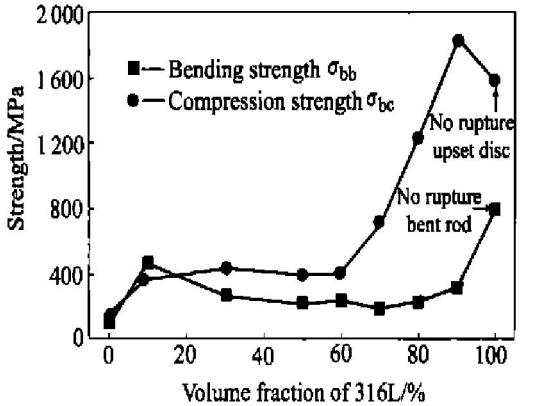

Fig. 6 Relationship between strength and volume fraction of 316L

The variation of bending strength σ_{bb} with the variation of 316L proportion is also shown in Fig. 6. In summary, the bending strength of samples with 10% to 70% proportion of 316L decreases slightly with the increase in 316L proportion, while that of samples from 80% 316L rises with the increase in 316L proportion. Owing to the harder stress state than in compressive testing, the samples in bending test show rather brittle, and low

strength value compared to that of the compressive strength, except for the case of 100% 316L samples, which are not broken down. The reason is that the framework composed of 316L particles by means of inter-bonding and coalescence and coarsening is relatively weak. As shown in Fig. 7, the fracture morphology of the bending test indicates 316L particle pullout in the cases of below 50% 316L and the rupture of framework composed of 316L particles by means of inter-bonding, coalescence and coarsening in the cases of above 60% 316L.

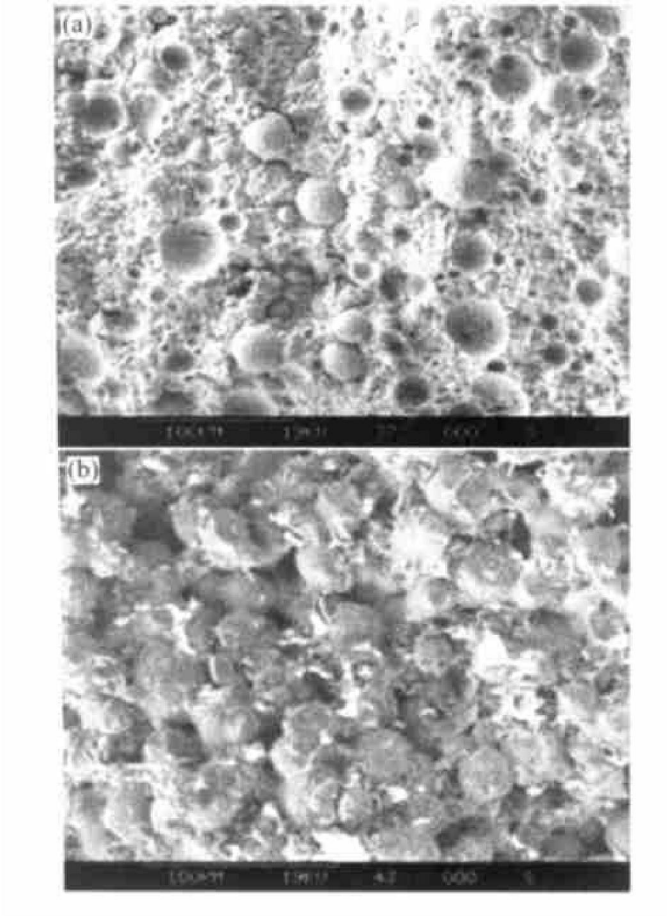

Fig. 7 Fracture morphologies of bending test
(a) —30% 316L; (b) —90% 316L

3.4 Electrical resistivity ρ

The variation of electrical resistivity ρ with the variation of 316L proportion is shown in Fig. 8, whereas, the samples of 0%, 10% and 30% 316L are non-conductive. Since the inter-bonding, coalescence and coarsening of 316L particles do not arise until the 316L proportion increases to 50%. The integrated framework of the 316L particles do not form until the 316L proportion increases to 60%, so the transient point of the electrical resistivity is approximately equal to 60% proportion of 316L. The results are consistent with the above microstructure and fracture morphology of the bending test. Moreover, the variation of the thermal conductivity with the variation of 316L proportion might be deduced according to that of the electrical resistivity[12-16], which is important to the optimum design to the composition and structure of multi-layer hollow functionally gradient materials.

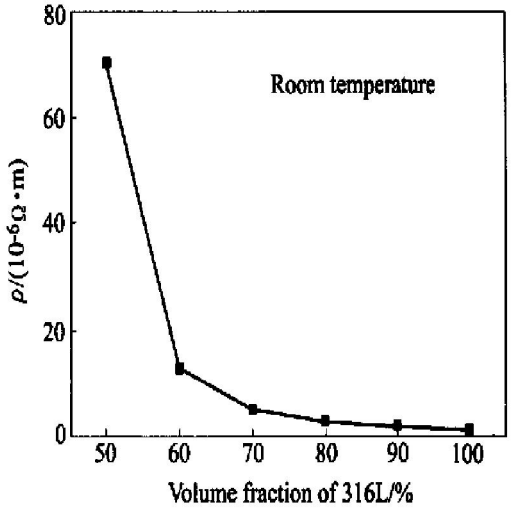

Fig. 8 Relationship between electrical resistivity ρ and volume fraction of 316L

Because of the relatively low sintering temperature for the densification of the PSZ, the sintered samples of PSZ do not reach full densification. Therefore, further works will try to utilize high-energy ball milling, higher sintering pressure, re-sintering, activated sintering, temperature gradient sintering, etc methods that might improve the microstructure and properties of the sintered samples.

4 CONCLUSIONS

1) The relative density of composites rises with the increase in 316L proportion, the results are relatively similar to those of as-extruded rods.

2) Matrix is PSZ in the samples with less than 60% 316L, and matrix is 316L in those with more than 60% 316L. Threshold of metallic matrix composite(MMC) is approximately equal to 60% 316L.

3) Micro-Vickers hardness of PSZ matrix rises gradually up to 30% 316L, then drops gradually, while $HMV_{0.2/15}$ of 316L particles varies unnoticeably over the whole range of 316L proportion.

4) The compression strength rises with the increase in 316L proportion. In contrast, the bending strength of samples with 10% to 70% 316L decreases slightly with the increase in 316L proportion, while that of the samples from 80% 316L rises with the increase in 316L proportion.

5) The electrical resistivity decreases with the increase in 316L proportion, whereas, samples of 0%, 10% and 30% 316L are non-conductive. The transient

point of electrical resistivity is approximately equal to 60% 316L.

REFERENCES

[1] Niino M, Hirai T, Watanabe R. Functionally gradient materials aimed at heat resisting materials for space plane [J]. J Jpn Soc Compos Mater, 1987, 13(6): 257 - 264. (in Japanese)

[2] ZHENG Zhi-qiao, LIANG Shu-quan, TAN Cheng-yu, et al. Functionally gradient materials aimed at ultra-heat resistance for astronautical area [J]. Technology of Astronautical Materials, 1992(6): 17 - 22. (in Chinese)

[3] Kawasaki A, Watanabe R. Powder metallurgical fabrication of the thermal-stress relief type of functionally gradient materials[A]. Somiya S, Shimada M, Watanabe R. Proceedings of the 4 th International Symposium on Science and Technology of Sintering, Vol. 2[C]. Tokyo, Japan: Elsevier Applied Science, 1987. 1197 - 1202.

[4] Sasaki M, Hirai T. Fabrication and properties of functionally gradient materials [J]. J Ceram Soc Jpn, Int Ed, 1991, 99(10): 970 - 980. (in Japanese)

[5] Gasik M. Principles of functionally graded materials[A]. Proceedings of 1998 Powder Metallurgy World Congress, Vol. 5[C]. European Powder Metallurgy Association, Granada, 1998. 357 - 362.

[6] Kawasaki A, Watanabe R. Concept and P/M fabrication of functionally gradient materials [J]. Ceram Int, 1997, 23(1): 73 - 83.

[7] XIE Jian-xin, ZUO Tie-yong, CHEN Zhong-chun, et al. New forming process of composite materials: multi-billet extrusion method [J]. Chinese Journal of Materials Research, 1995, 9(Suppl): 652 - 657. (in Chinese)

[8] CHEN Zhong-chun, XIE Jian-xin, Murakami T, et al. Fabrication of two-layer pipes composed of ZrO_2 and stainless steel by powder multi-billet extrusion method [J]. J Jpn Soc Technol Plasticity, 1995, 36(416): 1003 - 1008. (in Japanese)

[9] CHEN Zhong-chun, XIE Jian-xin, Murakami T, et al. Flow behavior of zirconia and stainless steel powder-binder compounds in extrusion [J]. J Jpn Soc Technol Plasticity, 1996, 37(425): 647 - 652. (in Japanese)

[10] CHEN Zhong-chun, XIE Jian-xin, Murakami T, et al. Effect of particle size distribution on extrusion characteristics of stainless steel powders containing binder [J]. J Jpn Soc Technol Plasticity, 1996, 37(425): 653 - 658. (in Japanese)

[11] XIE Jian-xin, CHEN Jing-ping, LIU Hui-nan. Extrusion characteristics of composite powders of stainless steel and zirconia [J]. Journal of University of Science and Technology Beijing, 1997, 19(6): 590 - 594. (in Chinese)

[12] NAN Ce-wen, CHEN Xin-zheng. Percolation model of Ti-Al_2O_3 cermet [J]. Acta Physica Sinica, 1987, 36(4): 511 - 513. (in Chinese)

[13] NAN Ce-wen, ZHANG Lian-meng, YUAN Run-zhang. Percolation phenomena in functionally gradient materials [J]. Journal of the Chinese Ceramic Society, 1993, 21(3): 272 - 274. (in Chinese)

[14] FAN Qiu-lin, HU Xing-fang, GUO Jing-kun. Mechanism of thermal and electrical conductivity on submicrostructural Ni-ZrO_2 composite [J]. Science in China(Series A), 1995, 25(7): 777 - 784. (in Chinese)

[15] FAN Qiu-lin, HU Xing-fang, GUO Jing-kun. Calculating method of the equivalent thermal conductivity of functionally gradient materials [J]. Journal of Inorganic Materials, 1997, 12(1): 115 - 120. (in Chinese)

[16] FAN Qiu-lin, XIAO Xing-cheng, HU Xing-fang, et al. Calculating method of the equivalent thermal conductivity of functionally gradient materials [J]. Materials Science and Engineering, 1999, A261: 84 - 88.

(Edited by PENG Chao-qun)